Supporting Information

Characterization of One-Electron Oxidized Copper(II)-Salophen-Type Complexes; Effects of Electronic and Geometrical Structures on Reactivities

Kazutaka Asami,[a] Akiko Takashina,[b] Misato Kobayashi,[c] Satoshi Iwatsuki,[c] Tatsuo Yajima,[d] Amélie Kochem,[e] Maurice van Gastel,[e] Fumito Tani,[f] Takamitsu Kohzuma,[b] Fabrice Thomas[g] and Yuichi Shimazaki *[a]

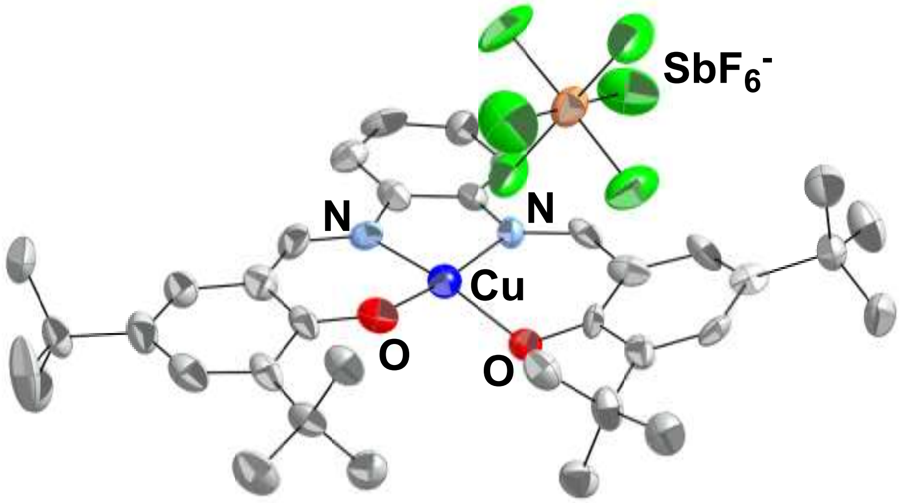

Fig. S1. Crystal structure of complex **[1]SbF$_6$** in the crystal of 2:1 mixture of **[1]SbF$_6$** and **1**, **[1]$_3$(SbF$_6$)$_2$**.

Table S1. Crystal data for complexes **[1]$_3$(SbF$_6$)$_2$** and **[2]SbF$_6$**.

	[1]$_3$(SbF$_6$)$_2$	**[2]SbF$_6$**
Formula	$C_{61}H_{76}N_3O_3Cu_{1.5}SbF_6$	$C_{31}H_{36}N_2O_4CuSbF_6Cl_2$
Formula weight	1230.35	1021.18
Color	brown	brown
Crystal size / mm	0.12 X 0.01 X 0.01	0.08 X 0.05 X 0.01
Crystal system	monoclinic	triclinic
Space group	$C2/c$	P-1
a (Å)	33.657(3)	10.8962(17)
b (Å)	17.489(1)	12.008(2)
c (Å)	19.991(2)	13.632(3)
α (°)	-	89.710(4)
β (°)	96.718(3)	81.617(4)
γ (°)	-	84.038(4)
V (Å^3)	11686(1)	1755.0(5)
Z	8	2
μ (Mo Kα) (cm^{-1})	10.68	15.97
F(000)	5084.00	872.00
D_{calc}(g/cm^3)	1.399	1.648
$2\theta_{\mathrm{max}}$ (°)	55.0	55.0
No. reflections obsd.	13357	7965
No. reflections used.	13357	7965
No. variables	681	422
R_1 $\{I > 2\sigma(\mathrm{I})\}^a$	0.0525	0.0857
R_w^{b}	0.1686	0.2547

[a] $R_1 = \Sigma||F_o| - |F_c|| / \Sigma|F_o|$ for $I > 2\sigma(I)$ data. [b] $R_w = \{\Sigma\omega(|F_o| - |F_c|)^2 / \Sigma\omega F_o^2\}^{1/2}$; $\omega = 1 / \sigma^2(F_o) = \{\sigma^{\square}{}_c(F_o) + p^2/4\bullet F_o^2\}^{-1}$.

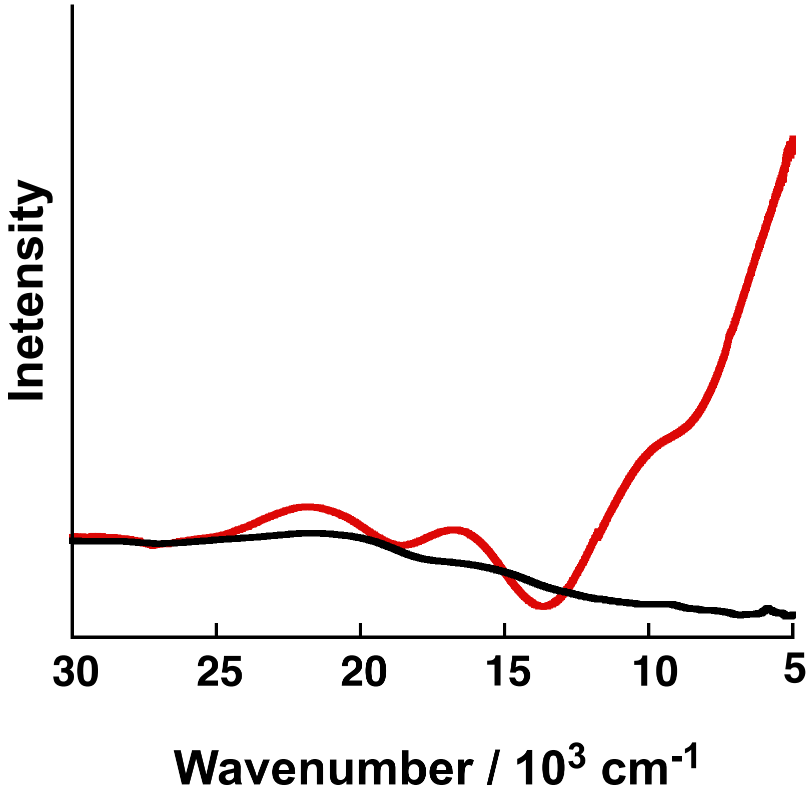

Fig. S2. Reflectance spectrum of complexes **1** and [**1**]**SbF$_6$**: black line: complex **1**; red line [**1**]**SbF$_6$**.

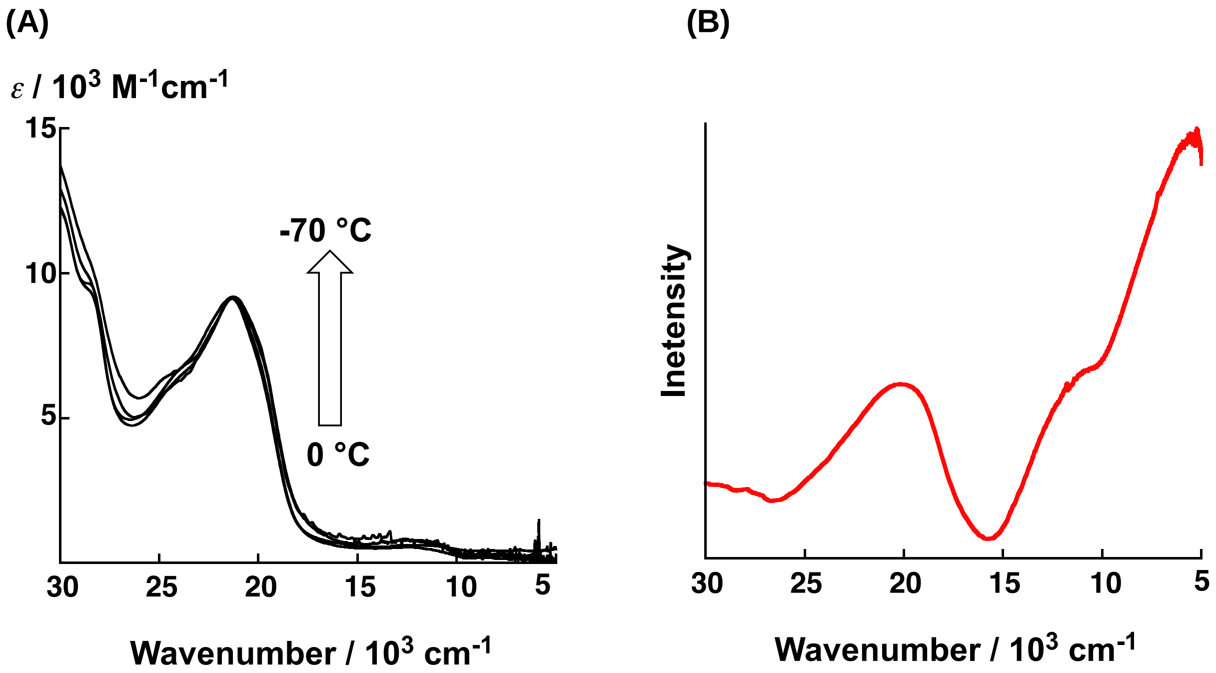

Fig. S3. UV-vis-NIR absorption spectra and reflectance spectrum of complex [**2**]**SbF$_6$**: (A) temperature-dependent UV-vis-NIR absorption spectral changes in CH_2Cl_2; (B) Reflectance spectrum of the solid sample.

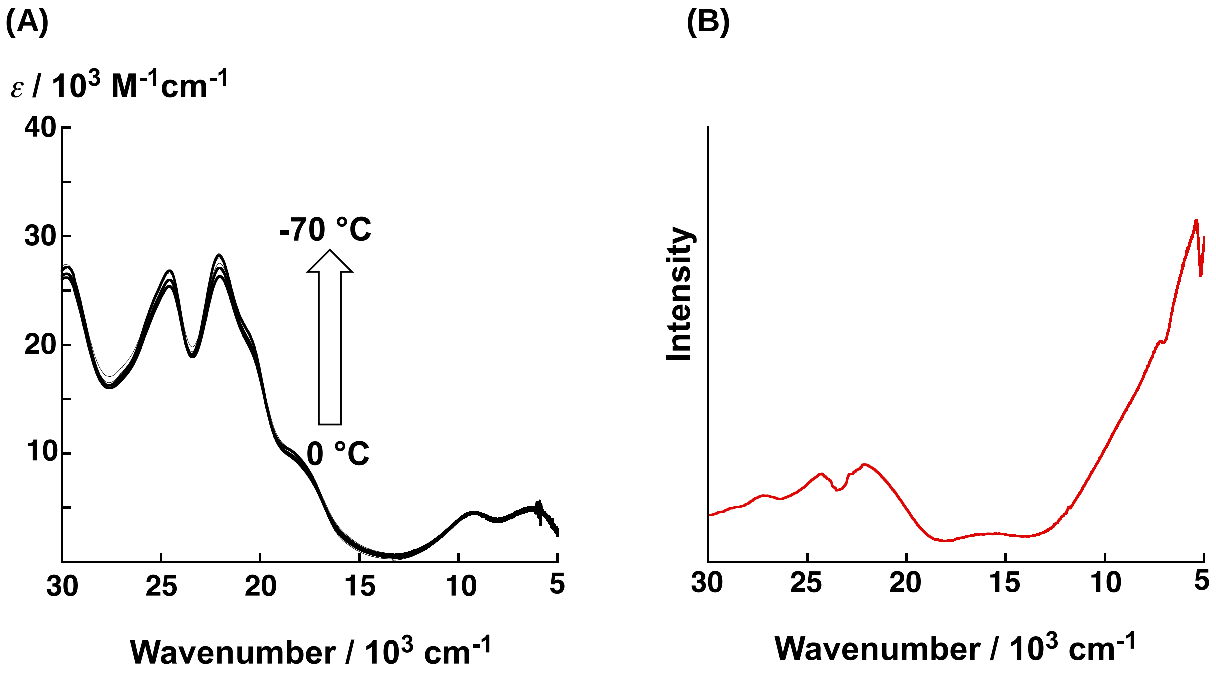

Fig. S4. UV-vis-NIR absorption spectra and reflectance spectrum of complex [**3**]**SbF$_6$**: (A) temperature-dependent UV-vis-NIR absorption spectral changes in CH_2Cl_2; (B) Reflectance spectrum of the solid sample.

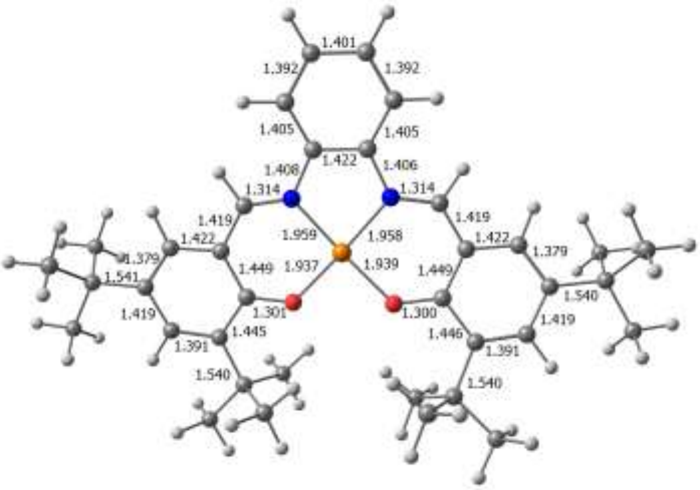

Fig. S5. Geometry optimized structure of **1** and selected bond distances.

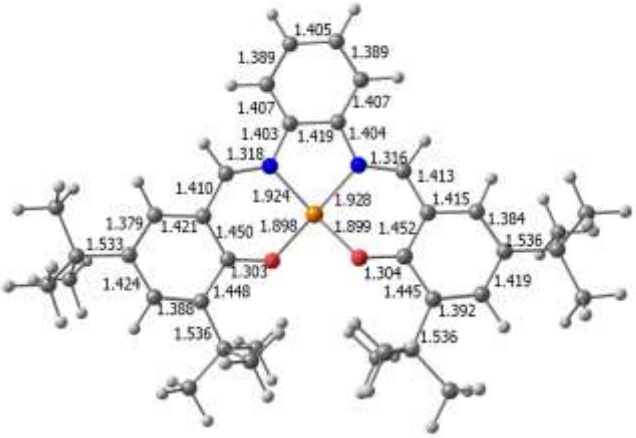

Fig. S6. Geometry optimized structure of **1**$^+$ and selected bond distances in the singlet state.

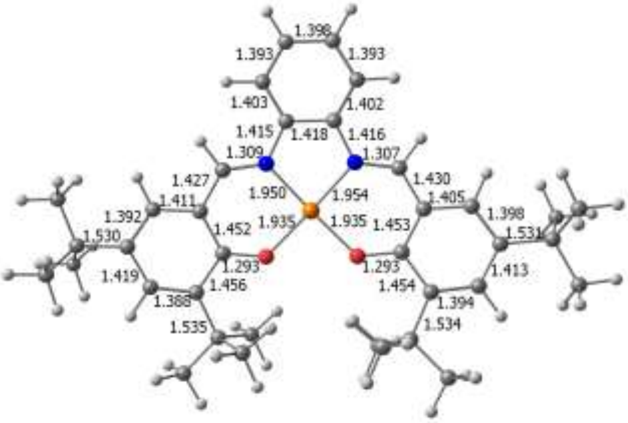

Fig. S7. Geometry optimized structure of **1**$^+$ and selected bond distances in the triplet state.

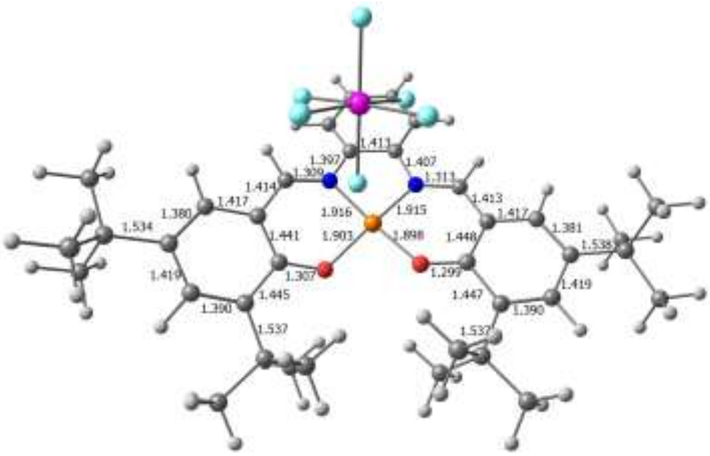

Fig. S8. Geometry optimized structure of **[1]SbF$_6$** and selected bond distances in the singlet state.

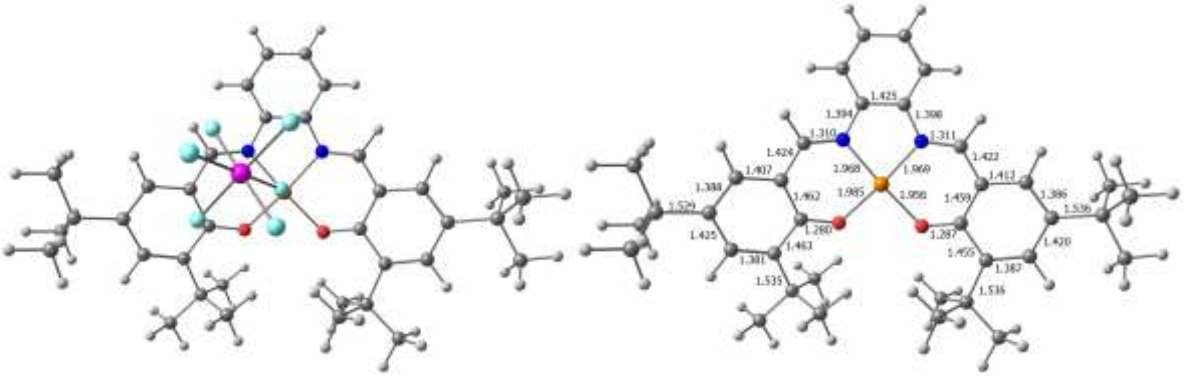

Fig. S9. Geometry optimized structure of **[1]SbF$_6$** in the triplet state and selected bond distances (counter ion removed for clarity).

Table S2. Observed pseudo first-order rate constants ($k_{\mathrm{obs}}{}^{\mathrm{1st}}$) for the reaction of **[1]**$^+$ with benzyl alcohol, α-benzyl-d_2 alcohol and benzyl alcohol-d under various conditions.

T / ºC	[Cu]$_0$/mM[a]	[alcohol]/M	10^3 $k_{\mathrm{obs}}{}^{\mathrm{1st}}$ / s^{-1} [b]
Reaction of **[1]**$^+$ with benzyl alcohol ($C_6H_5CH_2OH$)			
35.0	0.40	1.0	2.75, 2.82, 2.73
30.0	0.40	1.0	2.06, 2.06, 2.03
25.0	0.40	1.0	1.51, 1.52, 1.54
20.0	0.20	1.0	1.18, 1.19
20.0	0.40	1.0	1.11, 1.16, 1.17, 1.10, 1.12, 1.12
20.0	0.40	0.8	0.863, 0.910, 0.924
20.0	0.40	0.6	0.637, 0.653, 0.652
20.0	0.40	0.4	0.389, 0.396, 0.395
20.0	0.40	0.2	0.151, 0.167, 0.163
20.0	0.40	0.1	0.0661, 0.0738, 0.0718
15.0	0.40	1.0	0.795, 0.817, 0.837
10.0	0.40	1.0	0.593, 0.587, 0.613
Reaction of **[1]**$^+$ with α-benzyl-d_2 alcohol ($C_6H_5CD_2OH$)			
20.0	0.40	1.0	0.0895 (KIE = 13)
Reaction of **[1]**$^+$ with benzyl alcohol-d ($C_6H_5CH_2OD$) [c]			
20.0	0.40	1.0	1.16 (KIE = 1.0)

[a] Initial concentration of complex **[1]**$^+$.

[b] The $k_{\mathrm{obs}}{}^{\mathrm{1st}}$ was determined by nonlinear least-squares fitting of the following equation for first-order reactions to the change in the absorbance at 582 nm with time for 4-half lives of the decrease of the complex.

$$A_t = A_\infty + (A_0 - A_\infty)\exp(-k_{\mathrm{obs}}{}^{\mathrm{1st}}t)$$

[c] More than 80% deuterated.

Table S3. Observed pseudo second-order rate constants (k_{obs}^{2nd}) for the reaction of **[2]**$^+$ with benzyl alcohol, α-benzyl-d_2 alcohol and benzyl alcohol-*d* under various conditions.

T / °C	$[Cu]_0$/mM[a]	[alcohol]/M	k_{obs}^{2nd} / M^{-1} s^{-1} [b]
Reaction of **[2]**$^+$ with benzyl alcohol ($C_6H_5CH_2OH$)			
35.0	0.40	1.0	1.40
30.0	0.40	1.0	1.07
20.0	0.40	1.0	0.851, 0.708, 0.855, 0.767
20.0	0.40	0.8	0.574, 0.650, 0.587
20.0	0.40	0.6	0.416, 0.467, 0.422
20.0	0.40	0.4	0.273, 0.256, 0.271
20.0	0.40	0.2	0.0849, 0.101, 0.129
20.0	0.40	0.1	0.0459, 0.0443
15.0	0.40	1.0	0.658
Reaction of **[2]**$^+$ with α-benzyl-d_2 alcohol ($C_6H_5CD_2OH$)			
20.0	0.40	1.0	0.824 (KIE = 1.0)
Reaction of **[2]**$^+$ with benzyl alcohol-*d* ($C_6H_5CH_2OD$) [c]			
20.0	0.40	1.0	0.711 (KIE = 1.1)

[a] Initial concentration of complex **[2]**$^+$.

[b] The k_{obs}^{2nd} was determined by nonlinear least-squares fitting of the following equation for second-order reactions to the change in the absorbance at 800 nm:

$$A_t = A_\infty + (A_0 - A_\infty)/(1 + k_{obs}^{2nd}[Cu]_0 t)$$

where A_t and A_∞ are the absorbances at time t and ∞, respectively.[S1]

[c] More than 80% deuterated.

Table S4. Observed pseudo first-order rate constants ($k_{\mathrm{obs}}^{\mathrm{1st}}$) corresponding to the oxidation step for the reaction of **[3]**$^+$ with benzyl alcohol, α-benzyl-d_2 alcohol and benzyl alcohol-d under various conditions.

T / °C	$[\mathrm{Cu}]_0$/mM[a]	[alcohol]/M	$10^4\ k_{\mathrm{obs}}^{\mathrm{1st}}$ / s^{-1} [b]
Reaction of **[3]**$^+$ with benzyl alcohol ($C_6H_5CH_2OH$)			
35.0	0.20	1.0	6.32, 7.14, 7.10
30.0	0.20	1.0	3.76, 3.80
25.0	0.20	1.0	2.24, 2.43
20.0	0.20	2.2	1.77
20.0	0.20	1.8	1.76
20.0	0.20	1.4	1.61
20.0	0.20	1.0	1.41, 1.45, 1.70, 1.43, 1.46, 1.45, 1.51
20.0	0.20	0.8	1.32, 1,50
20.0	0.20	0.6	1.30, 1.47
20.0	0.20	0.4	1.22, 1.16, 1.11
15.0	0.20	1.0	0.966
10.0	0.20	1.0	0.548, 0.678
Reaction of **[3]**$^+$ with α-benzyl-d_2 alcohol ($C_6H_5CD_2OH$)			
20.0	0.20	1.0	0.997 (KIE = 1.5)
Reaction of **[3]**$^+$ with benzyl alcohol-d ($C_6H_5CH_2OD$) [c]			
20.0	0.20	1.0	1.34 (KIE = 1.1)

[a] Initial concentration of complex **[3]**$^+$.

[b] The $k_{\mathrm{obs}}^{\mathrm{1st}}$ was determined by nonlinear least-squares fitting of the following equation for consecutive 2-step reactions to the change in the absorbance at 582 nm:

$$A_t = A_\infty + \alpha \cdot \exp(-k_{\mathrm{obs}}^{\mathrm{1st}} t) + \beta \cdot \exp(-k_{\mathrm{dis}} t)$$

where k_{dis} is the rate constant for the disappearing process of the aldehyde after the aldehyde formation, A_t and A_∞ are the absorbances at time t and ∞, respectively, and α and β are composite parameters.[S2]

[c] More than 80% deuterated.

References in Tables S3 and S4

[S1] J. H. Espenson, "*Chemical Kinetics and Reaction Mechanisms*", 2nd ed.; McGraw-Hill, New York, 2002.

[S2] R. G. Wilkins, "*Kinetics and Mechanism of Reactions of Transition Metal Complexes*", 2nd ed.; VCH, Weinheim, Germany, 1991.

Table S5. Activation parameters for the benzyl alcohol oxidation with one-electron oxidized Cu(II)-salophen-type complexes.[a]

Complex	$\Delta H^{‡}$ /kcal mol^{-1}	$\Delta S^{‡}$ /cal mol^{-1}K^{-1}	$\Delta G^{‡}$(293K) /kcal mol^{-1}	E_a /kcal mol^{-1} [b]
[1]$^+$	10.0±0.1	-37.8±0.4	21.1±0.2	10.6±0.1
[2]$^+$	5.8±0.8	-39.2±2.7	17.5±1.6	6.4±0.8
[3]$^+$	16.2±0.5	-20.6±1.7	22.2±1.0	16.8±0.5
1,2-salcn [c]	10.2	-34.8	20.4	10.8
1,3-salcn [c]	10.7	-35.6	21.2	11.3

[a] Determined by the dependence of the observed rate constants at [$C_6H_5CH_2OH$] = 1.0 M ($k_{obs}^{1st\text{-}1M}$ for **[1]**$^+$ and **[3]**$^+$, and $k_{obs}^{2nd\text{-}1M}$ for **[2]**$^+$) on temperature. [b] Determined from Arrhenius analyses. [c] Ref. 22.

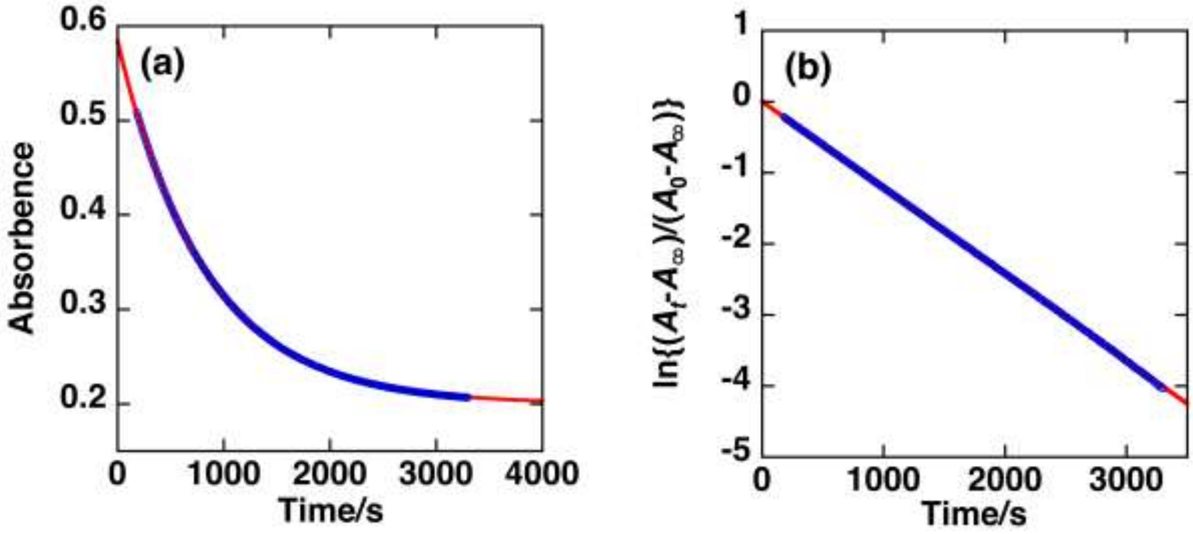

Fig. S10. (a) Absorbance change with time at 582 nm for the reaction of complex **[1]**$^+$ (0.40 mM) with benzyl alcohol (1.0 M). (b) The plot of $\ln\{(A_t - A_\infty)/(A_0 - A_\infty)\}$ against time. The linearity of the plot indicates that this system obeys first-order kinetics.

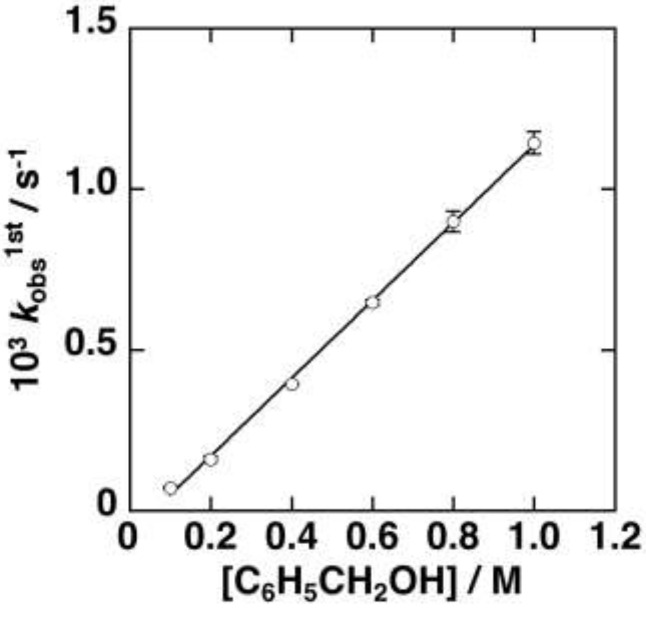

Fig. S11. The dependence of the observed pseudo first-order rate constant (k_{obs}^{1st}) on the concentration of excess substrate for the reaction of **[1]**$^+$ with benzyl alcohol at 293 K. The data are shown with a linear fit (slope = (1.21 ± 0.02) x 10^{-3} M^{-1} s^{-1}, intercept = (–0.07 ± 0.01) x 10^{-3} s^{-1}).

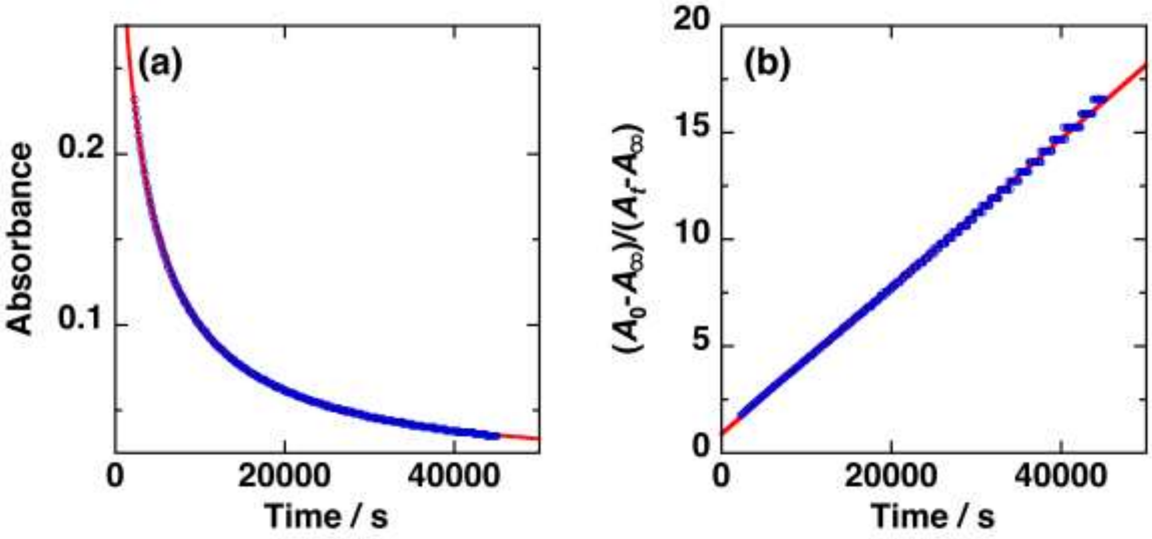

Fig. S12. (a) Absorbance change (at 800 nm) with time for the reaction of complex **[2]**$^+$ (0.40 mM) with benzyl alcohol (1.0 M). (b) The plot of $(A_0 - A_\infty)/(A_t - A_\infty)$ against time. The linearity of the plot indicates that this system obeys second-order kinetics.

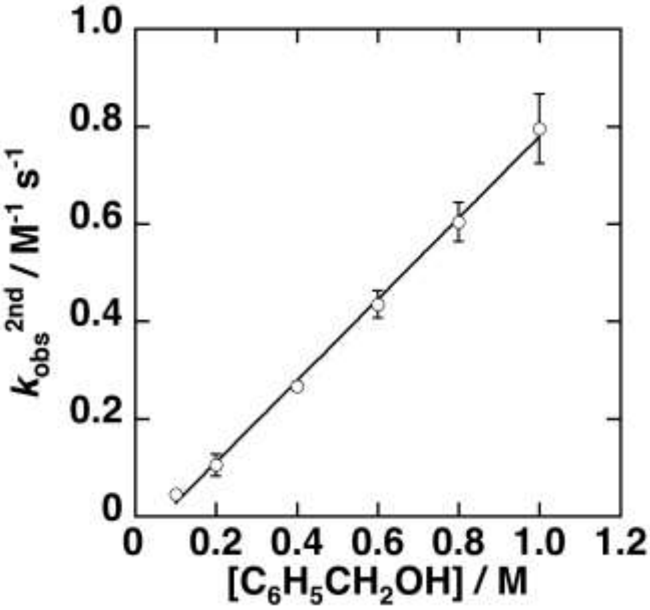

Fig. S13. The dependence of the observed pseudo second-order rate constant (k_{obs}^{2nd}) on the concentration of excess substrate for the reaction of **[2]**$^+$ with benzyl alcohol at 293 K. The data are shown with a linear fit (slope = 0.84 ± 0.03 M^{-2} s^{-1}, intercept = –0.06 ± 0.02 M^{-1} s^{-1}).

Detailed description of kinetic analyses for the reaction of [3]$^+$ with benzyl alcohol

The absorbance change with time for the reaction of complex **[3]**$^+$ with benzyl alcohol showed a 2-step first-order reaction in the presence of a large excess concentration of $C_6H_5CH_2OH$ over the total concentration of **[3]**$^+$ (**Fig. S14**). GC-MS analyses revealed that the first reaction step (k_{obs}^{1st}) corresponds to the aldehyde formation. The k_{obs}^{1st} was determined by nonlinear least-squares fitting of the following equation for consecutive 2-step reactions to the change in the absorbance at 582 nm:

$$A_t = A_\infty + \alpha\cdot\exp(-k_{obs}^{1st}t) + \beta\cdot\exp(-k_{dis}t)$$

where A_t and A_∞ are the absorbances at time t and ∞, respectively, and α and β are composite parameters.[S2]

Reference

[S2] R. G. Wilkins, "*Kinetics and Mechanism of Reactions of Transition Metal Complexes*", 2nd ed.; VCH, Weinheim, Germany, 1991.

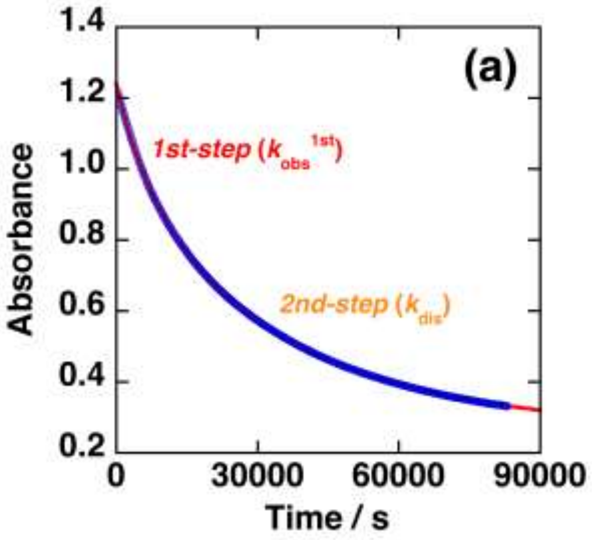

Fig. S14. (a) Absorbance change (at 582 nm) with time for the reaction of complex **[3]**$^+$ (0.20 mM) with benzyl alcohol (1.0 M). (b) Semi-log ($\log|A_\infty - A_t|$ vs. time) plot (blue) indicates that this system obeys consecutive 2-step first-order kinetics, in which the first step corresponds to the aldehyde formation process which was confirmed by GC-MS analysis.

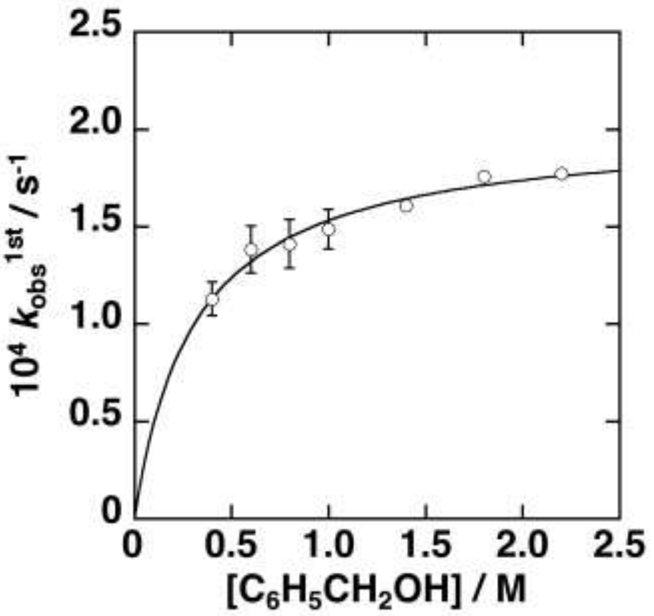

Fig. S15. The dependence of the observed pseudo first-order rate constant (k_{obs}^{1st}) on the concentration of excess substrate for the reaction of **[3]**$^+$ with benzyl alcohol at 293 K. The data are shown with a saturated fit based on $k_{obs}^{1st} = Kk_1[C_6H_5CH_2OH]/(1 + K[C_6H_5CH_2OH]$ ($k_1 = (1.9 \pm 0.1) \times 10^{-4}$ s^{-1} and $K = 3.7 \pm 0.7$ M^{-1}).

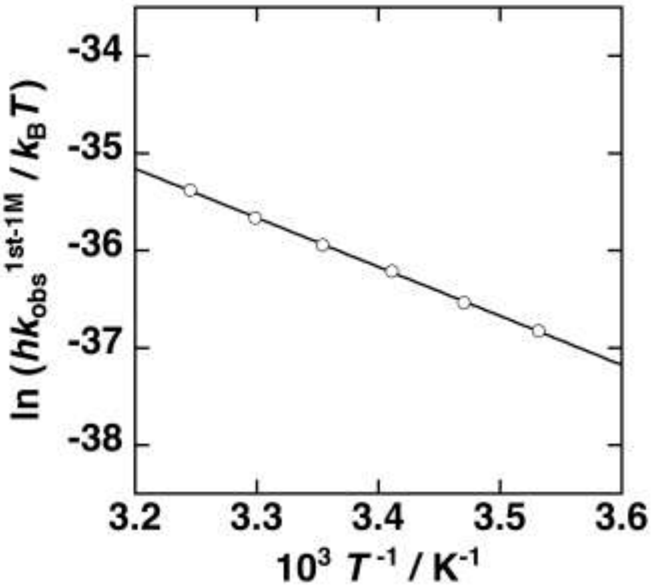

Fig. S16. Eyring plot of the conditional pseudo first-order rate constant at [$C_6H_5CH_2OH$] = 1.0 M ($k_{obs}^{1st\text{-}1M} = k_2$) for the reactions of complex **[1]**$^+$ with benzyl alcohol.

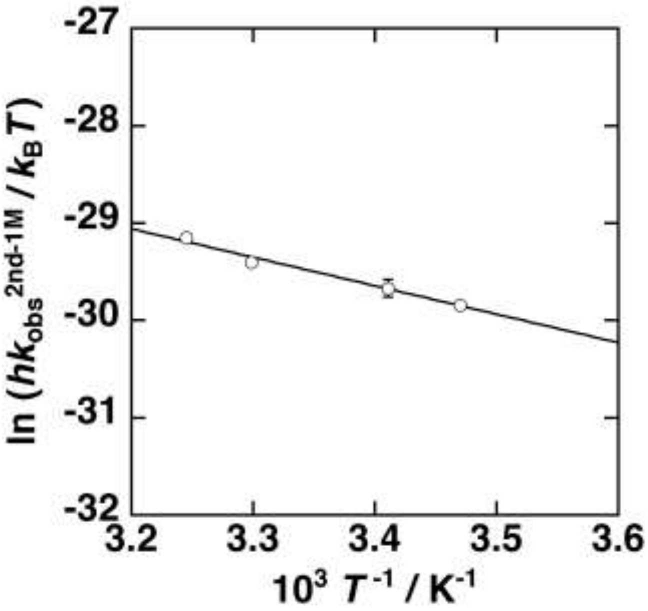

Fig. S17. Eyring plot of the conditional pseudo second-order rate constant at [$C_6H_5CH_2OH$] = 1.0 M ($k_{obs}^{2nd\text{-}1M} = k_3$) for the reactions of complex **[2]**$^+$ with benzyl alcohol.

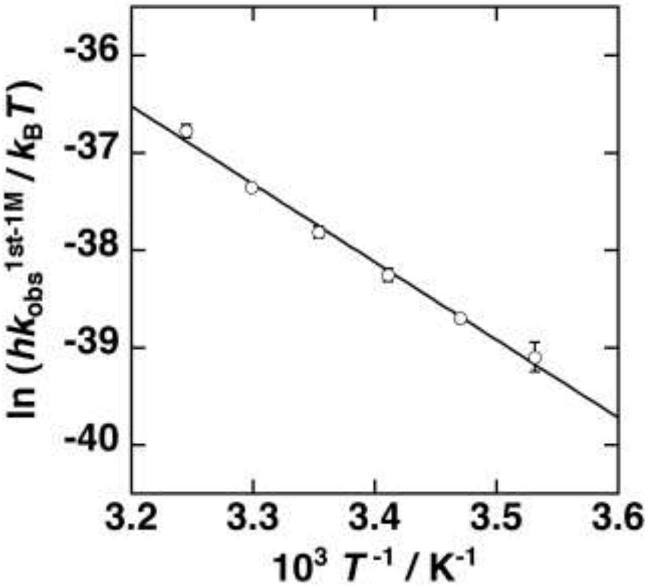

Fig. S18. Eyring plot of the conditional pseudo first-order rate constant at [$C_6H_5CH_2OH$] = 1.0 M ($k_{obs}^{1st\text{-}1M} = k_1K/(1+K)$) for the reactions of complex **[3]**$^+$ with benzyl alcohol.